Figure 2-b portrays the effect of shifting the origin of the three-port, by $\delta_{1,2,3}$, on the real part of the normalized transfer impedance of the perforate i.e., $\Re$. $\Re$ is determined under excitation from all three ducts to give $\Re_1$, $\Re_2$, and $\Re_3$, respectively. In absence of these added alterations, calculated as per Eq. (2), a clear difference in the behavior of the resistance curves under excitation from different directions is observed. Moreover, in case of excitations from ducts 1 and 2, the resistance appears to be negative for frequencies >1100 Hz, suggesting incorrect results without the addition of the calculated alterations.

As mentioned in Section II-A, to validate the accuracy of the plane wave decomposition over the perforated section a comparison of resistance is done, as shown in Figure 2 Figure 2-c. Calculation of $\Re$ is done using Eq. (3), where in one case the value of total acoustic pressure at P_0 is measured using a microphone, and in the other case it is taken as the average of the decomposed wave amplitudes in duct 1 and 2, which are evaluated at P_0. Moreover, determination of $\Re$ is also done by taking the difference of calculated resistance with and without the perforate present in the T-junction. The resistance calculated using all the above-mentioned three methods exhibit good agreement. Given the small deviation over the frequency range, plane wave decomposition can be used for the determination of the sound field in the perforated section. The large deviations observed in the resistance curves, e.g., at ≈ 520, 1150 Hz can be attributed to the experimental errors caused due to standing wave patterns in the duct.

A comparison between the normalized resistance calculated using Eqs. (3) to (6) is shown in Figure 2Figure 2-d. It should be noted that for frequencies >1100 Hz, the resistance values calculated by Eq. (3) under excitation from ducts 1 and 2 are smoothened by using the S-Matrix coefficients. This is due to the removal of the effect of the termination reflections, and subsequently the measurement error due to the presence of nodes near the position P_0. A good agreement is observed between all the calculation methods, the model proposed in Eq. (7), and the resistance calculated from the impedance tube measurements [20].

B. Flow Profile Results

Figure 3 a) Flow profile measurements using pitot tube; b) Comparison between the measured and the modelled flow velocity profiles Figure 3 displays the measured flow Mach Numbers. The displayed measurement data are the average of the values determined at three different positions with respect to the perforate. An empirical model for the measured profile is proposed in Eq. (12).**(12)**

$$\begin{aligned} u(x) &= 0.0145x^+ + \beta, && for\ 11 < x^+ < 350\ in\ the\ buffer\ layer \\ \frac{u(x)}{u_\tau} &= \frac{1}{0.384} ln(x^+) + 4.27, && for\ 350 < x^+ < 830\ in\ the\ logarithmic\ layer \\ \frac{u_{max} - u(x)}{u_\tau} &= 6.3\left(\frac{x}{H/2}\right)^2, && for\ 830 < x^+\ in\ the\ outer\ zone \end{aligned} \tag{12}$$

where $x^+ = \frac{xu_\tau}{\nu}$ is the normalized distance from the hard wall, u_{max} is the maximum velocity (observed at the center of the cross section), and β is a constant determined by curve fitting of the measured data. The limits of x^+ for the buffer and the logarithmic layer are defined using Ref. [30] and [31].

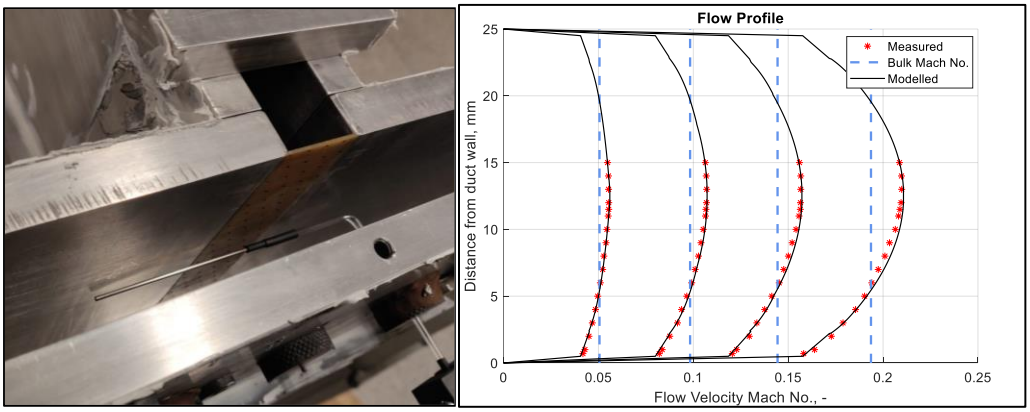

Figure 3 a) Flow profile measurements using pitot tube; b) Comparison between the measured and the modelled flow velocity profiles

Based on Eqs. (10) and (11), the skin friction velocity along with the different flow profile characteristics were calculated as shown in Table 1Table 1.

Mach Number	u_{max} (m/s)	u_{bulk} (m/s)	u_τ (m/s)	δ^* (mm)	θ (mm)
0.05	19.19	17.21	0.90	9.44	2.25
0.1	36.99	33.33	1.63	6.62	3.05
0.14	54.22	48.92	2.28	3.94	2.64
0.19	72.68	65.55	2.96	1.08	0.90

Table 1 Flow profile characteristics

C. Three port results under grazing flow

The magnitude of the S-Matrix coefficients and the normalized resistance calculated in the presence of grazing flow is as shown in Figure 4 Figure 4. On observing the scattering matrix coefficients, it can be clearly seen that with increasing flow velocity, the transmission from and into the duct 3 decreases and its reflection increases. This effect is due to an increase in the overall resistance of the perforate.

As displayed in Figure 4 Figure 4-b, as the flow speed increases, the resistance calculated under acoustic excitation from the grazing direction i.e., $\Re_{1,2}$ increase. Moreover, an increase in the flow speeds also show the resistance becoming increasingly independent of the frequency. The behavior of the curves starts following the Rao and Munjal model [26]. However, under incidence from duct 3, the resistance curve i.e., $\Re_3$ displays a dependence on the frequency as well as the flow speed, following the behavior seen in Ref. [21]. The reason for the discrepancy of the resistance under normal and grazing incidence with increasing flow speeds is unknown.

Moreover, on comparing with the results from impedance eduction methods [10], it is found that the distinguishing behavior of the resistance curves under upstream and downstream excitation is absent in the three-port results presented here. However, the behavior portrayed under normal incidence is similar to that of the resistance calculated using impedance eduction under downstream incidence.

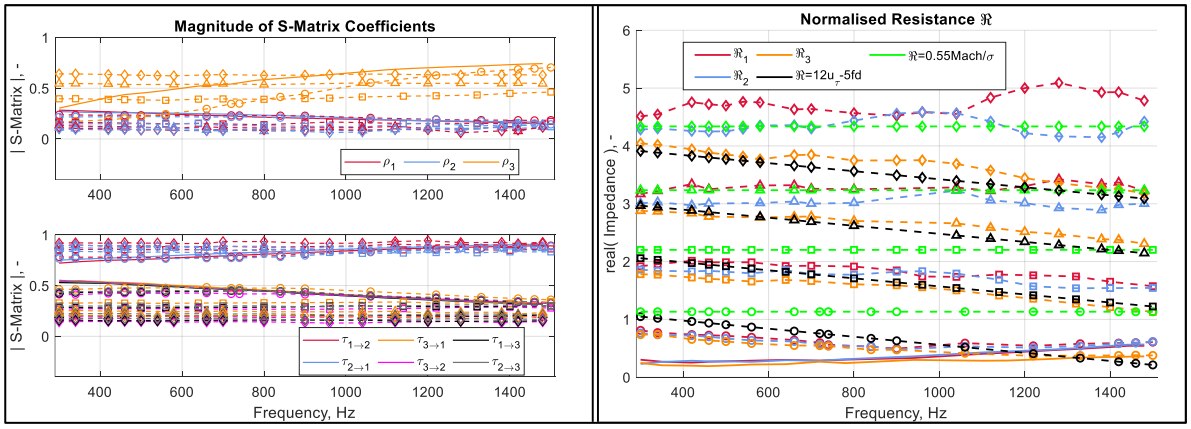

Figure 4 a) Magnitude of S-Matrix coefficients in presence of grazing flow; b) Normalized resistance calculated in the presence of external flow compared against proposed models, solid lines: No grazing flow, circles: Mach No. ≈ 0.05, squares: Mach No. ≈ 0.1, triangles: Mach No. ≈ 0.14, diamonds: Mach No. ≈ 0.19.

A modification to the semi-empirical model of Kooi and Sarin [21] is proposed to match the experimental results of calculated resistance. Resistance calculated as per Eq. (13) agrees well with the experimental results under normal acoustic incidence as can be seen in Figure 4 Figure 4-b. Similarly, modifying Rao and Munjal [26], Eq. (14) describes the resistance calculated under grazing incidence at higher flow speeds of Mach No. ≈ 0.14 and 0.19,

$$\Re = \frac{12u_\tau - 5fd}{\sigma c} \tag{13}$$

$$\Re = \frac{0.55Mach}{\sigma} \tag{14}$$

In order to understand the flow acoustic interaction effect on the properties of the test sample under normal incidence, the transmission coefficient and the resistance of the empty T-Junction were calculated with grazing flow and the results were compared. Scaling of the experimentally determined quantities with respect to the flow speeds was done by using Strouhal number (St) which is calculated using Eq. (15).

$$St = {}^{f d_{eq}}/_{U}, \tag{15}$$

where U is taken as the bulk flow velocity, and d_{eq} is taken as the equivalent diameter of the rectangular pipes in case of an empty T-Junction. When the sample is placed in the T-junction, d_{eq} is taken as the diameter of the perforations. It should be noted that the diameter and the thickness of the perforated sample under consideration is equal, hence the length scaling factor is calculated using only the diameter in the analysis of the sample.

The transmission coefficients as well as the resistance of the empty T-junction calculated under normal acoustic incidence at all flow speeds is shown in Figure 5 Figure 5-a. As observed in Ref. [17], the transmission coefficients of the empty T-junction show oscillating variation with respect to the Strouhal number, indicating amplification and attenuation of the incident sound at particular Strouhal numbers. The Strouhal numbers where an amplification is displayed corresponds to intervals where the calculated resistance decreases to negative values as shown in Figure 5 Figure 5-b. Moreover, it can also be seen that the Strouhal numbers at which the resistance values equal zero are 2^n multiples of a principle Strouhal number, i.e., the resistance decreases to cross zero at $St \approx 0.44, 0.86, 1.67$.

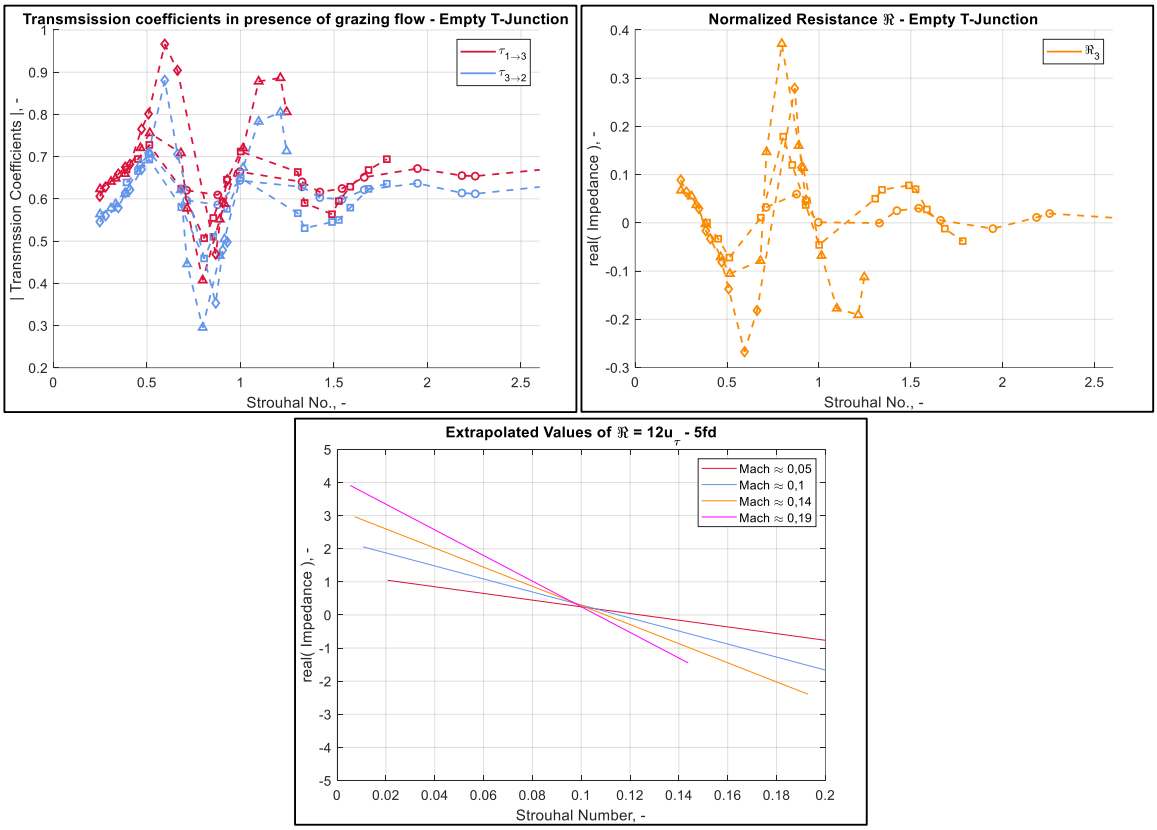

Figure 5 a) Magnitude of the transmission coefficients of the empty T-Junction; b) Normalised resistance of the Empty T-junction calculated under normal acoustic incidence; circles: Mach No. ≈ 0.05, squares: Mach No. ≈ 0.1, triangles: Mach No. ≈ 0.14, diamonds: Mach No. ≈ 0.19; c) Extrapolation of resistance calculated using Eq. (13) to determine the zero resistance Strouhal number.

To compare with the perforated sample, Figure 5 Figure 5-c shows the extrapolated resistance of the perforated plate. This extrapolation is done adhering to Eq. (13), with the aim of determining the Strouhal number where the resistance of the perforated sample in presence of grazing flow becomes zero. The Strouhal Number is determined to be roughly 0.11. In case of the empty T-junction experiments, for the given frequency range all the determined

Strouhal numbers are > 0.25. On expanding the frequency range to include lower Strouhal numbers, if a fundamental is observed at $St \approx 0.11$, it suggests a similarity in the flow-acoustic field of an empty T-junction and a perforate under normal acoustic incidence. Moreover, in case of the perforate an approach towards an oscillating behavior, like the one observed in the empty T-junction, can also be investigated by expanding the Strouhal Number range. If observed, these similarities in the flow-acoustic field under normal acoustic incidence can be the reason for the behavior of the perforate resistance curve.

IV. Concluding Remarks

To study the transfer impedance of a perforated plate, an experimental three-port technique is presented in this study. Using the three-port, the acoustic properties of the perforate are studied with and without the presence of grazing flow, and under acoustic incidence from the normal and the grazing directions. To reduce the errors occurring due to termination reflections, incorporation of the scattering matrix coefficients in the calculation of the transfer impedance is displayed. In the absence of flow, agreement between the calculated resistance and an existing analytical model is found. On the addition of grazing flow, determination of the flow profile characteristics is carried out. A clear dependency of the flow velocity on the value of normalized resistance is seen and the resemblance between the behavior of the three-port results and existing semi-empirical models is shown. Modifications in the constants of the existing models are suggested to fit the experimental results. Similarities in the flow-acoustic field of an empty T-junction and a perforated section are shown. Moreover, a possible reason for the behavior of the calculated resistance curve under normal acoustic incidence is proposed. Future works include expanding the Strouhal number range to study the possibly oscillating amplification and attenuation by the perforate sample, and study the discrepancy observed in the calculated resistance under excitation from normal and grazing directions.

Acknowledgments

This work is part of the Marie Skłodowska-Curie Initial Training Network Pollution Know-How and Abatement (POLKA). We gratefully acknowledge the financial support from the European Commission under call H2020-MSCA-ITN-2018 (project number: 813367).

References

[1] Jones, M. G., Parrott, T. L., and Watson, W. R., *Comparison of Acoustic Impedance Eduction Techniques for Locally-Reacting Liners*, in *9th AIAA/CEAS Aeroacoustics Conference*. 2003: Hilton Head, South Carolina. p. 1837-1847.

[2] Watson, W. R. and Jones, M. G. , *Comparison of Convected Helmholtz and Euler Model for Impedance Eduction in Flow*, in *12th AIAA/CEAS Aeroacoustics Conference*. 2006: Cambridge, Massachusetts.

[3] Jones, M.G., Watson, W.R., and Nark, D.M., *Effects of Flow Profile on Educed Acoustic Liner Impedance*, in *16th AIAA/CEAS Aeroacoustics Conference*. 2010: Stockholm, Sweden.

[4] Jones, M.G. , Watson, W.R., Howerton, B.M. and Busse-Gerstengarbe, S., *Comparative study of Impedance Eduction Methods, art 2: NASA Tests and Methodology*, in *19th AIAA/CEAS Aeroacoustics Conference*. 2013.

[5] Watson, W.R., and Jones, M. G, *A Comparative Study of Four Impedance Eduction Methodologies Using Several Test Liners*, in *19th AIAA/CEAS Aeroacoustics Conference*. 2013: Berlin, Germany.

[6] Elnady, T., Bodén, H., and Elhadidi, B., *Validation of an Inverse Semi-Analytical Technique to Educe Liner Impedance.* AIAA Journal, 2009. **47**: p. 2836-2844.

[7] Busse-Gerstengarbe, S., Richter, C., Lahiri, C., Enghardt, L., Roehle, I., Thiele, F., Ferrante, P., and Scofano, A., *Impedance Eduction Based on Microphone Measurements of Liners under Grazing Flow Conditions.* AIAA Journal, 2012. **50**: p. 867-879.

[8] Zhou, L., Bodén, H., Lahiri, C., Bake, F., Enghardt, L. and Elnady, T., *Comparison of impedance eduction results using different methods and test rigs*, in *20th AIAA/CEAS Aeroacoustics Conference*. 2014: Atlanta, GA.

[9] Kabral, R., Bodén, H. and Elnady, T., *Determination of Liner Impedance under High Temperature and Grazing Flow Conditions*, in *20th AIAA/CEAS Aeroacoustics Conference*. 2014: Atlanta, GA.

[10] Bodén, H., Zhou, L., Cordioli, J., Medeiros, A. and Spillere, A., *On the effect of flow direction on impedance eduction results*, in *22nd AIAA Aeroacoustics Conference*. 2016.

[11] Dean, P.D., *An In-Situ method of wall acoustic impedance measurements in flow ducts.* Journal of Sound and Vibration, 1974. **34**: p. 97-130.

[12] Zandbergen, T., *On the Practical Use of Three-Microphone Techniqe for In-Situ Acoustic Impedance Measurements on Double Layer Flow Duct Liners*, in *7th AIAA Aeroacoustics Conference*. 1981.
[13] Gaeta, R.J., Mendoza J.M. and Jones M.G., *Implementation of in-situ impedance techniques on a full scale aero-engine system*, in *13th AIAA Aeroacoustics Conference*. 2007.
[14] Dickey, N.S., Selamet, A. and Ciray, M.S., *An experimental study of the impedance of perforated plates with grazing flow.* Journal of Acoustical Society of America, 2001. **110**: p. 2360-2370.
[15] Feder, E. and Dean, L. W., *Analytical and Experimental Studies for Predicting Noise Attenuation in Acoustically Treated Ducts for Turbofan Engines NASA Contractor Report CR-1373* 1969.
[16] Karlsson, M. and Åbom, M., *Aeroacoustics of T-junctions-an experimental investigation.* Journal of Sound and Vibration, 2010. **329**: p. 1793-1808.
[17] Holmberg, A., Karlsson, M. and Åbom, M., *Aeroacoustics of rectangular T-junctions subject to combined grazing and bias flows - An experimental investigation.* Journal of Sound and Vibration, 2015. **340**: p. 152-166.
[18] Myers, M.K., *On the Acoustic Boundary Condition in the presence of Flow.* Journal of Sound and Vibration, 1980. **71**: p. 429-434.
[19] Guess, A.W., *Calculation of Perforated Plate Liner Parameters from Specified Acoustic Resistance and Reactance.* Journal of Sound and Vibration, 1975. **40**: p. 119-137.
[20] Shah S., Bodén H. and Boij, S., *Experimental Study on the Acoustic Properties of Perforates under Flow using Three-Port Technique*, in *27th International Congress on Sound and Vibration*. 2021 (unpublished).
[21] Kooi, J.W. and Sarin, S.L., *An experimental study of the acoustic impedance of Helmholtz resonator arrays under a turbulent boundary layer*, in *7th AIAA Aeroacoustics Conference*. 1981.
[22] Rice, E.J. , *A Model for the acoustic impedance of a perforated plate liner with multiple frequency excitations* 1971.
[23] Åbom, M. and Bodén, H. , *Error analysis of two-microphone measurements in ducts with flow.* Journal of Acoustical Society of America, 1988. **83**: p. 2429-2438.
[24] Kirby, R. & Cummings, A., *The impedance of perforated liners subjected to grazing flow and backed by porous media.* Journal of Sound and Vibration, 1998.
[25] Cummings, A., *The effects of Grazing Turbulent Pipe-Flow on the Impedance of an Orifice.* Acoustica, 1986. **61**: p. 233-242.
[26] Rao, N. and Munjal, M., *Experimental evaluation of Impedance of perforates with Grazing Flow* Journal of Sound and Vibration, 1986.
[27] Zanoun, E-S, Nagib,H. and Durst, F., *Refined cf relation for turbulent channels and consequences for high-Re experiments.* Fluid Dynamics Research, 2009. **41**.
[28] Schlichting, H., *Boundary Layer Theory*. 1968: McGraw-Hill Inc.
[29] Dokumaci, E., *A Note on Transmission of Sound in a Wide Pipe with Mean Flow and Viscothermal Attenuation.* Journal of Sound and Vibration, 1997. **208**: p. 653-655.
[30] Lee, M. and Moser, R., *Direct numerical simulation of turbulent channel flow up to $Re_\tau \approx 5200$.* Journal of Fluid Mechanics, 2015. **774**: p. 395-415.
[31] Zhou, L., *Acoustic characterization of orifices and perforated liners with flow and high-level acoustic excitation*, in *MWL Sound and Vibration*. 2015, KTH Royal Institute of Technology.